STATISTICAL STUDY OF RELATIONSHIPS BETWEEN DAYSIDE HIGH-ALTITUDE/-LATITUDE O^+ OUTFLOWS, SOLAR WINDS, AND GEOMAGNETIC ACTIVITY

Sachiko Arvelius[1], M. Yamauchi[1], H. Nilsson[1], R. Lundin[1], H. Rème[2], M. B. Bavassano-Cattaneo[3], G. Paschmann[4], A. Korth[5], L. M. Kistler[6], and G. K. Parks[7]

[1]*Swedish Institute of Space Physics (IRF), Box 812 SE-981 28 Kiruna, Sweden*
[2]*Centre d'Etude Spatiale des Rayonnements, Toulouse, France*
[3]*Instituto di Fisica dello Spazio Interplanetario, Roma, Italy*
[4]*International Space Science Institute, Bern, Switzerland*
[5]*Max-Planck-Institut für Sonnensystemforschung, Katlenburg-Lindau, Germany*
[6]*University of New Hampshire, Durham, USA*
[7]*Space Science Laboratory, UC Berkeley, USA*

ABSTRACT

The terrestrial origin O^+ outflow, which is persistently observed by the Cluster CIS/CODIF instrument, was studied statistically in succession in the dayside high-altitude (from 5 up to 11 R_E) and high-latitude (from 75 to 90 degrees invariant latitude, deg ILAT) region. We extended the previous study (Arvelius et al., 2005a), investigating correlations between the properties (namely, maximum or 'dominant' differential particle flux, $MDPF$, and its energy, PE) of dayside high-altitude polar outflowing O^+, solar winds (solar wind moments and the interplanetary magnetic field, IMF, conditions), and local mid-/low-latitude geomagnetic activity (measured by ASY/SYM indices). In this study, we found firstly that energization and/or acceleration of dayside high-altitude polar outflowing O^+ is(are) controlled by both strong southward IMF (defined by intensity, B_t, and clock angle, θ. in this case, $|\theta|>135°$) and solar wind moments (except solar wind electric field), but it(they) occur(s) at two different places: one is the poleward cusp and/or the mantle region controlled by the IMF, the other is the entire polar cap controlled by the solar wind moments. Secondarily outflowing O^+ flux enhancement and O^+ keV energization/acceleration process(es) are different in terms of occurence time scale and location, even tough both are controlled by solar winds and the IMF. Thirdly both energization/acceleration and flux enhancement of dayside high-altitude and high-latitude outflowing O^+ correlate to local mid-/low-latitude geomagnetic activity (as measured by ASY/SYM indices), i.e. higher energy of outflowing O^+ appears at higher altitudes and more equatorward (a similar trend to that of the K_p index (Arvelius et al., 2005a)), and flux enhancement of outflowing O^+ appears at lower altitudes and more poleward. However the correlation is not as clear as the case of the IMF conditions / the solar wind parameters.

Key words: Solar wind-magnetosphere interactions; Magnetosphere-ionosphere coupling; O^+energization/acceleration; O^+outflow..

1. INTRODUCTION

The previous study (Arvelius et al., 2005a) is extended in this study in terms of correlations between the properties of dayside high-altitude and high-latitude outflowing O^+, solar winds (IMF conditions and moments), and local mid-/low-latitude geomagnetic activity. The correlations are investigated particularly with a "time-shifted" comparison at the time scale of from tens of minutes to an hour.

The data set of dayside high-altitude and high-latitude outflowing O^+ is provided by the Cluster CIS/CODIF instrument. We selected 129 Cluster traversals in the dayside polar region (year of 2001-2003, from January to May), and the observation points are counted to more than 80,000. The data set utilized in this study is the same as that in the previous study (Arvelius et al., 2005a). A sample data is shown in Figure 1.

1.1. Previous results

The results from the previous study (Arvelius et al., 2005a) are shown in Figure 2 and Figure 3. We concluded that (1) the latitudinal distribution of outflowing O^+ in

Proceedings Cluster and Double Star Symposium – 5th Anniversary of Cluster in Space, Noordwijk, The Netherlands, 19 - 23 September 2005 (ESA SP-598, January 2006)

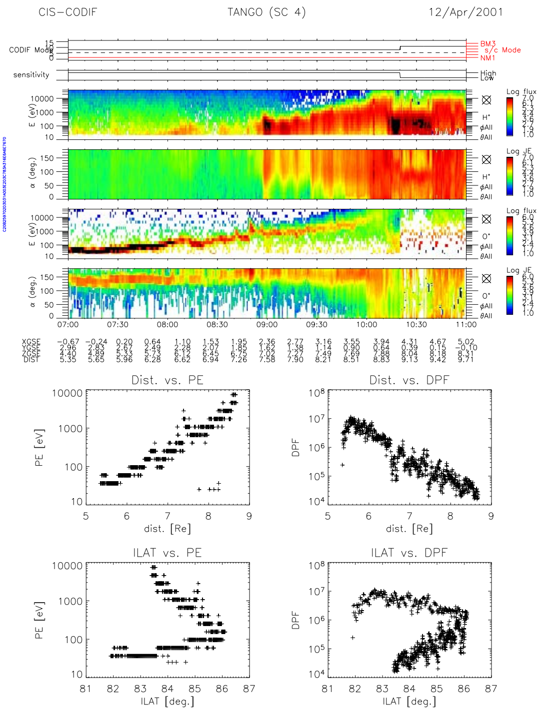

Figure 1. A Sample data on 12 April, 2001. (Upper) The 3rd-6th panels from the top are a time-energy spectrogram of H$^+$ in the unit of flux [part/(cm^2·sec·sr·keV)], a time-pitch angle distributions (PADs) of H$^+$ in the unit of energy flux, JE [keV/(cm^2·sec·sr·keV)], a time-energy spectrogram and time-PADs of O$^+$, respectively. We identified field-aligned upward-going O$^+$ by sight, e.g. selecting the time interval between 07:00-10:00 UT from the upper figure. (Bottom) The properties of outflowing O$^+$ (the energy of maximum differential particle flux, termd by PE, and the maximum differential particle flux, termed by $MDPF$) as functions of geocentric distance (R_E) and deg ILAT. In the figure, 670 observation points are plotted.

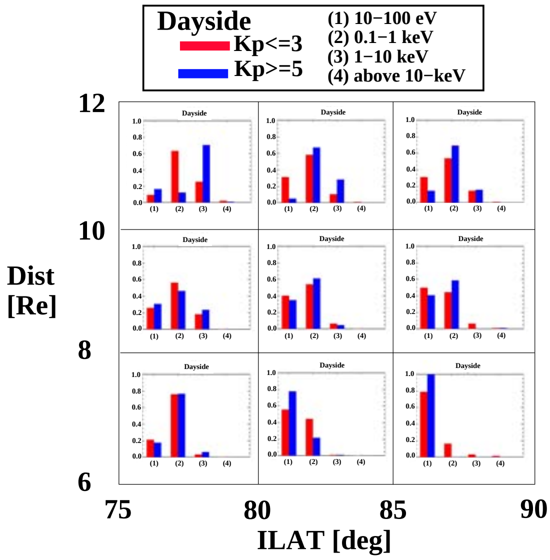

Figure 2. PE occurrence rates of different PE levels in the dayside polar region. The whole region (6–12 R_E geocentric distance and 75–90 deg ILAT) is divided into $2R_\mathrm{E}\times5°$ subregions. The pairs of bars in each panel denote $K_p\leq3$ (in red) and $K_p\geq5$ (in blue), ordered in horizontal line from the left-hand side, (1) 10$\leq PE<$100 eV, (2) 0.1$\leq PE<$1.0 keV, (3) 1.0$\leq PE<$10 keV, and (4) $PE\geq$10 keV.

terms of peak energy, i.e. PE, is consistent with velocity filter dispersion at 6-8 R_E geocentric distance (or below 8 R_E geocentric distance), while that of above 8 R_E geocentric distance cannot be explained by velocity filter effect only, and that (2) a tendency to observe outflowing keV O$^+$ is obvious for $K_p\geq5$ than $K_p\leq3$ at higher altitudes.

Concerning above (1), we suggest additional energization and/or acceleration mechanism(s) of outflowing O$^+$ in the dayside high-altitude and high-latitude region. Two candidates examined in the previous paper are (a) centrifugal force and (b) ponderomotive force, and both of them might contribute to energy gain of outflowing keV O$^+$ partially, but not be major process.

On the other hand, the result (2) above indicates that higher K_p is in general related to strong magnetospheric convection, however, as shown in the result (1) above, latitudinal distribution of outflowing keV O$^+$ ions cannot be explained by velocity filter effect, which is caused by the anti-sunward magnetospheric convection) only. Therefore we aim to examine correlations between the properties of dayside high-altitude and high-laitutde outflowing O$^+$ and the solar winds as well as geomagnetic activity as measured by ASY/SYM indices with high time resolution (1 minutes). In Figure 4 the definition of IMF B_x (anti-)parallel to the geomagnetic field and the legend of gray-scaled bar are shown.

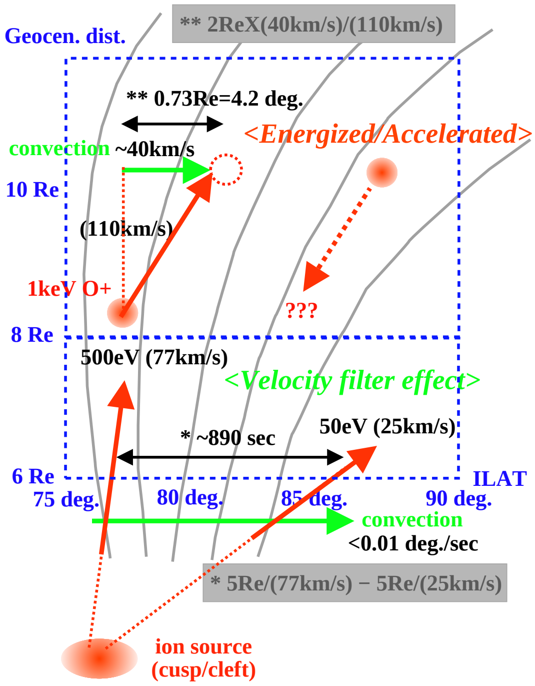

Figure 3. The schematic (not scaled) for interpreting Figure 3. This sketch shows that we can explain the latitudinal distribution of outflowing O$^+$ observed below 8 R_E geocentric distance by velocity filter effect, whereas that of outflowing O$^+$, in particular with more than 1 keV, observed above 8 R_E geocentric distance cannot be explained by velocity filter effect only. Therefore we suggest that additional energization and/or acceleration process(es) may take place at high altitudes. The potential candidates for outflowing O$^+$ energization/acceleration process are examined in the paper by Arvelius et al. (2005a). Note that effects by geomagnetic activity, e.g. K_p dependence, are not taken into account in this sketch.

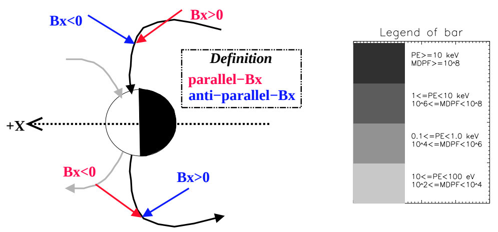

Figure 4. (Left) Definition of the IMF B_x which is "parallel to the geomagnetic field" ($B_{x,\parallel}$) or "anti-parallel to the geomagnetic field" ($B_{x,\nparallel}$) by schematic. (Right) The legend of gray-scaled bar adopted in this paper.

2. RESULTS

2.1. Solar wind dependences on PE

The spatial (both altitudinal and latitudinal) PE distribution of dayside high-latitude and high-latitude outflowing O$^+$ are examined in response to the IMF conditions / the solar wind moments at different time lags (60, 30, 20, and 10 minutes). The "time lag" means that the solar winds which are estimated to reach the subsolar point precede observing outflowing O$^+$ events by 60, 30, 20, and 10 minutes.

The optimum time lag for the best correlation is 10 minutes and the clearest correlation can be seen at the altitude interval of 10–12 R_E geocentric distance. The positive correlations can be seen for (a) strong southward IMF (clock angle, θ, is defined as $|\theta|>135°$) and (b) solar wind velocity x-component, V_x, while the negative correlations can be seen for (c) solar wind proton density, N_p and (d) solar wind dynamic pressure, P_{sw}. There is no correlation seen for the solar wind electric field ($E4$).

The latitudinal distributions of PE occurrence rates in response to (1) strong southward IMF, B_t ($|\theta|>135°$), (2) IMF B_x parallel to the geomagnetic field ($B_{x,\parallel}$), and the solar wind moments (3–6) are shown in Figure 5. As shown in Figure 5, the energization and/or acceleration of dayside high-altitude and high-latitude outflowing O$^+$ is controlled by the solar wind moments (N_p, V_x and P_{sw}) and the IMF conditions (B_t ($|\theta|>135°$)), however at two different places. One is the poleward cusp and/or the mantle region (below 80 deg ILAT) at higher altitude (i.e. 10–12 R_E geocentric distance) where the strong southward IMF influences. The other is the entire entire polar cap, in particular 80–85 deg ILAT, at vertically broader altitude intervals (i.e. above 8 R_E geocentric distance) where the solar wind moments influence dominantly.

2.2. Solar wind dependences on $MDPF$

The spatial distributions of $MDPF$ occurrence rates are also examined in response to the IMF conditions / the solar wind moments at different time lags (60, 30, 20, and 10 minutes). The optimum time lag for the best correlations is chiefly 60 minutes and the best correlations can be seen at the altitude interval of 6–8 R_E geocentric distance.

The positive correlations can be seen for (a) strong southward IMF, (b) IMF $B_{x,\parallel}$ but at the time lag of 10 minutes, (c) solar wind proton density, (d) solar wind dynamics pressure, and (e) solar wind electric field. The negative correlation can be seen only for the solar wind dynamic pressure at the time lag of 10 minutes.

The latitudinal distribution of $MDPF$ occurrence rates in response to (1) strong southward IMF, B_t ($|\theta|>135°$) at the altitude interval of 8–10 R_E geocentric distance, (2) P_{sw} (also representative for N_p), (3) $E4$, and (4) $B_{x,\parallel}$ at the time lag of 10 minutes are shown in Figure 6, respectively. The altitude interval chosen for (1) is due to a better statistics. As shown in Figure 6, flux enhancement of

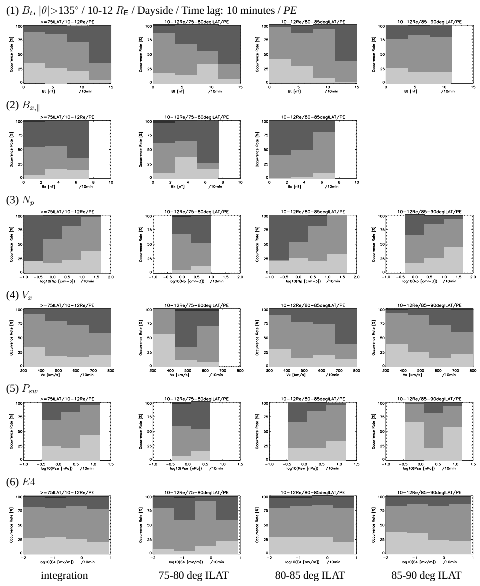

Figure 5. Latitudinal distribution of PE occurrence rates at the altitude interval of 10–12 R_E geocentric distance and at the time lag of 10 minutes. The left-most columns are latitudinal integration between 75–90 deg ILAT.

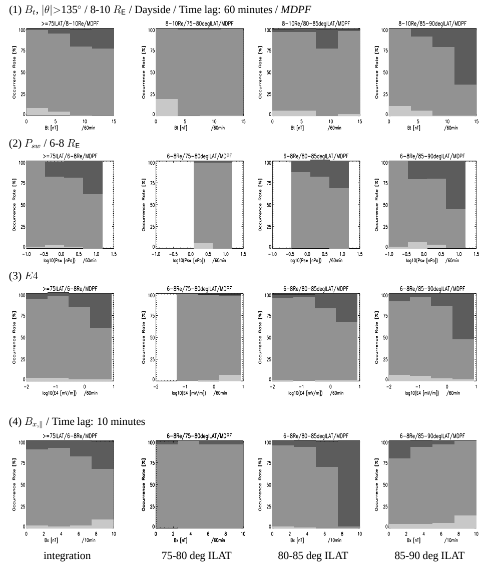

Figure 6. Latitudinal distribution of $MDPF$ occurrence rates at the altitude interval of 6–8 R_E geocentric distance (default) and at the time lag of 60 minutes (default). The left-most columns are latitudinal integration between 75–90 deg ILAT.

outflowing O^+ is also controlled by both the solar wind moments (N_p, P_{sw} and $E4$) and the strong southward IMF (B_t ($|\theta|$>135°)), however the optimum time lag and location for the best correlations are different from those in the case of outflowing keV O^+ energization and/or acceleration process(es). The optimum time lag is in principle 60 minutes. The location for the best correlations is at the altitude interval of 6–8 R_E geocentric distance and more poleward (i.e. 85–90 deg ILAT). Furthermore, this result indicates also that flux enhancement of outflowing O^+ is influenced by dynamics of the ionosphere.

2.3. Geomagnetic activity dependences

Both PE and $MDPF$ occurrence rates at different time lags (60, 40, and 20 minutes) in response to SYM-H and ASY-D indices are also examined.
The best correlations can be seen at different places for either PE or $MDPF$ occurrence rates of outflowing O^+: at the altitude interval of 10–12 R_E geocentric distance for PE, and at the altitude interval of 6–8 R_E geocentric distance for $MDPF$. These trends are similar to the cases for the solar winds, while independent of character of geomagnetic activity (i.e. large negative value of SYM-H index, e.g. less than -50 nT, indicates a ring current enhancement associated with geomagnetic storms, whereas large positive value of ASY-D index, e.g. more than 20–30 nT, indicates a east-west auroral electrojet intensification at the nightside associated with substorm onsets). Only the optimum time lag for the best correlations is different for SYM-H and ASY-D indices.
The spatial (both altitudinal and latitudinal) distributions of PE and $MDPF$ occurrence rates in response to ASY-D index at the time lag of 20 minutes are shown in Figure 7 and Figure 8. As shown in these figures, both energization/acceleration and flux enhancement of dayside high-altitude and high-latitude outflowing O^+ correlate to ASY-D index, i.e. higher energy of outflowing O^+ appears at higher altitudes and more equatorward, while flux enhancement of outflowing O^+ appears at lower altitudes and more poleward. The former trend is similar to the case for K_p index (Arvelius et al., 2005a). However these correlations are not as clear as those for the solar winds.

3. SUMMARY

We summarize this investigation and conclude as follows:

1. The energization and/or acceleration of dayside outflowing O^+ at high altitudes and high latitudes is directly (i.e. nearly immediately in time scale) controlled by solar winds. The processes occur at two places: one is at the high-altitude poleward and/or the mantle region controlled by the IMF, the other at the entire polar cap above 8 R_E geocentric distance controlled by the solar wind moments (N_p, V_x and P_{sw}, but not by $E4$).

2. The keV O^+ has a positive correlation to strong southward IMF and V_x, but a negative correlation to N_p and P_{sw}. There is no correlation between keV O^+ and the solar wind electric field ($E4$).

3. The energization and/or acceleration process(es) of dayside outflowing O^+ in which the energy level achieves more than 1 keV occurs locally at high altitudes. On the other hand, the flux enhancement of dayside outflowing O^+ occurs in the entire polar cap region and is strongly related to the dynamics of the ionosphere. These differences are confirmed by the investigation of optimum time lags for the best correlation to the solar wind moments / the IMF conditions.

4. The peak flux of dayside outflowing O^+ has a positive correlation to strong southward IMF, P_{sw}, and $E4$, which is fully consistent with other previous studies.

5. Both keV energization/acceleration and flux enhancement of dayside outflowing O^+ correlate to geomagnetic activity, i.e. higher energy outflowing O^+ appears at higher altitudes and more equatorward, and flux enhancement of outflowing O^+ appears at lower altitudes and more poleward. However these correlations to geomagnetic activity are not as clear as those to the solar winds.

The contents of this paper are excerpted from Arvelius et al. (2005b). The investigation of relationships between 3-hour-averaged solar wind parameters (including the IMF conditions) and K_p index has also been done and the results are described in Arvelius et al. (2005c).

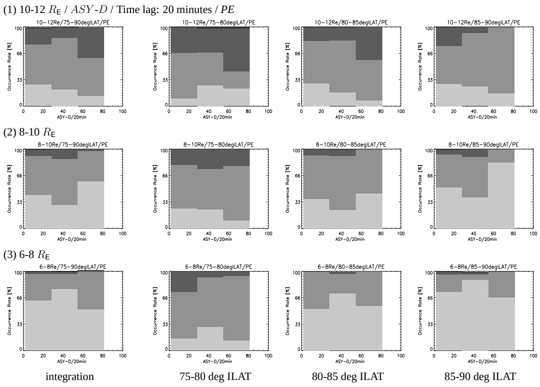

Figure 7. Spatial distribution of PE occurrence rates in response to ASY-D at the altitude interval of 10–12 R_E geocentric distance. The left-most panels are latitudinal integration between 75–90 deg ILAT.

ACKNOWLEDGEMENTS

We thank the Cluster/CIS instrument team and CNES (Toulouse, France) for providing the CIS data and data visualization tool. The K_p and ASY/SYM indices are distributed by the WDC C1 for Geomagnetism at DMI, Copenhagen, Denmark (data source is the WDC C2 for Geomagnetism, Kyoto, Japan). We thank the ACE-MAG/-SWEPAM instrument team and the ACE Science Center for providing the ACE level-2 data (combined MAG/SWEPAM, 64-second averaged).

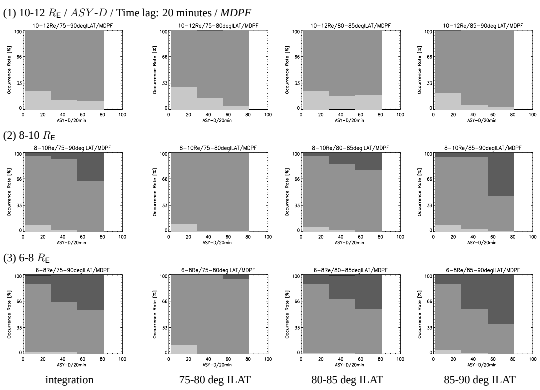

Figure 8. Spatial distribution of $MDPF$ occurrence rates in response to ASY-D at the altitude interval of 6–8 R_E geocentric distance. The left-most panels are latitudinal integration between 75–90 deg ILAT.

REFERENCES

Arvelius, S., Yamauchi, M., Nilsson, H., et al.: Statistics of high-altitude and high-latitude O^+ ion outflows observed by Cluster/CIS, *Ann. Geophys.*, **23**, 1909–1916, 2005a.

Arvelius, S., Yamauchi, M., Nilsson, H., et al.: Statistical study of relationships between dayside high-altitude and high-latitude O^+ ion outflows, solar winds, and geomagnetic activity, submitted to *Ann. Geophys.*, 2005b.

Arvelius, Sachiko: *Energization and Acceleration of Dayside Polar Outflowing Oxygen* (Doctoral thesis), IRF Scientific Report (in press), ISBN 91-7305-963-3, October, 2005c.